Preprints of the 21st IFAC World Congress (Virtual)
Berlin, Germany, July 12-17, 2020

Passive Fault-Tolerant Model Predictive Control of AC/DC PWM Converter in a Hybrid Microgrid

Saeedreza Jadidi *, Hamed Badihi *,, and Youmin Zhang *§**

** Department of Mechanical, Industrial and Aerospace Engineering, Concordia University, Montreal, Quebec, Canada (e-mails: saeedreza.jadidi@concordia.ca; youmin.zhang@concordia.ca)*

*** College of Automation Engineering, Nanjing University of Aeronautics and Astronautics (NUAA), Nanjing, Jiangsu, China (e-mail: hamed.badihi@nuaa.edu.cn)*

Abstract: This paper aims at presenting a novel fault-tolerant control (FTC) scheme for an AC/DC pulse-width modulation (PWM) converter operating in a microgrid framework. A group of interconnected loads and distributed renewable energy resources such as wind farm, solar photovoltaic (PV) farm, and a battery energy storage are considered to form a microgrid. The control system for the AC/DC PWM converter aims at tolerating the fault effects due to power-loss malfunctions in the solar system. A passive fault-tolerant control scheme based on model predictive control (MPC) is proposed and the effectiveness of the designed scheme is demonstrated in an advanced microgrid benchmark model implemented in MATLAB/Simulink environment.

Keywords: microgrid, renewable sources, fault-tolerant control, model predictive control, PWM converter.

1. INTRODUCTION

One of the key challenges facing the electricity sector is to meet the growing demand for electricity in a safe, secure and environmentally friendly way. For many years, utility companies have relied upon fossil fuels such as coal, oil and natural gas as the main sources of electricity production. However, such conventional sources suffer from several disadvantages such as adverse environmental impacts and limited resources. In addition to the mentioned issues, the existing power grid has several limitations. For instance, only about one third of fuel energy can be converted into electricity in traditional power plants. Also, a significant amount of electricity is lost along the extended transmission lines. Some other challenges relate to the aging infrastructures, nonoptimal usage of the assets, domino-effect failures and widespread blackouts due to the hierarchical topology of the system (Jadidi et al., 2019a).

One key solution to overcome the mentioned shortcomings of the conventional power grid is to create an 'intelligent' or 'smart' grid which integrates information technology and communication systems into the existing power grid. More precisely, *smart grid* is a cyber-enabled power grid which provides a bidirectional power and information flow to enable a comprehensive control and wide-area monitoring/protection over all distributed grid components. In addition, it facilitates the more efficient integration of intermittent renewable energies such as wind and solar into the power grid.

A smart grid is basically a network of smaller grid components called *smart microgrids*. As initially introduced in Lasseter (2001), a microgrid is a group of distributed energy resources (DERs) and loads which constitute a single controllable entity with the ability to operate in *grid-connected* and/or *islanded* modes. Certainly, the microgrid protection is one of the most critical issues regarding the reliability of microgrids. A well-designed protection system is necessary to detect and handle any fault conditions in microgrids. Indeed, protection systems suitable for use in microgrids are expected to be much more complicated and involved comparing with the currently available protection systems. This is particularly true since the energy in a microgrid can flow in different directions.

In microgrids, although different types of faults are possible to occur in different components, some faults can be effectively tolerated at the control system level. Generally speaking, conventional control methods cannot guarantee the stability of the system or a desirable performance under fault conditions in components such as actuators, sensors or other subsystems. To solve this problem, fault-tolerant control (FTC) systems are introduced which can maintain the overall performance (under fault conditions) by handling the fault effects. From a control system design point of view, there are two different types of FTC: active (AFTC) and passive (PFTC). AFTC systems use real-time fault detection and diagnosis (FDD) information and control reconfiguration to maintain the entire system stable and achieve an acceptable performance in the presence of faults (Badihi et al., 2019). On the contrary, PFTC systems are fixed controllers which are robust against some levels of faults in the system without using any FDD information or explicit control reconfiguration.

The specific application of FTC methods in microgrids is a relatively new topic of research which needs more investigation. In Gholami et al. (2018), a linear state-space model of a DER in grid-connected microgrids is described, and then, an AFTC system for sensor faults is designed using a sliding mode observer (SMO) as an FDD unit. In Youssef and Sbita (2017), adaptive observers are used for fault detection and isolation of the sensors in a three-phase inverter, and an AFTC method is introduced against faults in a photovoltaic system. An FTC strategy based on model predictive control (MPC) approach is presented in Prodan et al. (2015) for reliable operation of microgrid energy management unit. The problem of sensor failures in a wide-area measurement system due to

communication losses or sensor faults is considered in Khosravani et al. (2016). A hybrid wind-diesel-PV microgrid is simply modeled in Minchala-Avila et al. (2014), and two FTC methods based on MPC and adaptive control are designed against faults in a diesel engine generator. Also, applications of fuzzy logic on designing PFTC controllers for power electronic converters at the microgrid level are presented and discussed in Jadidi et al. (2019b).

This paper aims to present a novel PFTC scheme based on an MPC approach which is applied to an AC/DC pulse-width modulation (PWM) converter operating in a microgrid. The considered microgrid includes a group of interconnected loads and renewable DERs such as a wind farm (a group of wind turbines), a solar photovoltaic (PV) farm, and a battery energy storage system (BESS). Compared with the already cited works in the literature, this paper specifically targets power-loss faults in a microgrid's PV system and presents a PFTC scheme based on MPC to tolerate the fault effects. The effectiveness of the designed scheme is demonstrated in an advanced microgrid benchmark model implemented in MATLAB/Simulink environment.

The rest of the paper is organized as follows: Section 2 discusses the designed microgrid benchmark. Section 3 presents the considered PV power-loss fault and its effects on the microgrid performance. The design of PFTC scheme for the AC/DC converter is addressed in Section 4. Section 5 illustrates and discusses the simulation results. Lastly, the conclusions are drawn in Section 6.

2. MICROGRID BENCHMARK

This paper considers a cluster of loads and renewable DERs including a wind farm, a solar PV farm, and a BESS to form a hybrid AC/DC microgrid which can connect to or disconnect from a medium-voltage distribution power grid. A single-line diagram of the considered microgrid is shown in Fig. 1. As seen in this figure, the microgrid has two feeders which are connected to a 25kV bus. These feeders are equipped with circuit breakers (CBs) and power electronic converters to regulate the power flow. A microgrid central controller (MGCC) regulates the operation of the microgrid in both grid-connected and islanded modes of operation. An advanced nonlinear model of this microgrid benchmark is implemented in MATLAB/Simulink environment with a high level of precision and a wide variation in operating conditions. The sampling time of this dynamic model is assumed to be 5.05×10^{-6} sec (sufficiently lower than the propagation time of the system) and the total simulation time is 4 seconds.

In the benchmark, the wind farm component includes six wind turbines with three-phase doubly fed induction generators (DFIGs) each rating at 1.5-megawatt (MW) output power. The solar farm represents an array of PV modules which are designed to generate 100 kW of power in normal conditions depending on the solar radiation, cell temperature, and the number of interconnected cells and modules. Indeed, at any level of solar radiation, the maximum output power can be captured at a unique point on the current-voltage diagram of a solar cell. In order to generate power at this point, maximum power point tracking (MPPT) control is considered. The BESS is modelled as a dynamic model of a rechargeable lithium-ion battery according to Tremblay and Dessaint (2009). Since the mentioned DERs cannot directly integrate (connect) into the microgrid, appropriate power electronic interfaces are needed to enable safe DERs integrations. For instance, this benchmark employs a unidirectional DC/DC converter (with an internal MPPT control algorithm and a boost converter) for the integration of the PV array. Also, a bidirectional DC/DC converter including a battery controller is considered for the battery integration. Indeed, the power electronic devices such as AC/DC PWM converters improve the integration and controllability of these DERs.

Figure 2 shows a schematic of the implemented DC part of the hybrid microgrid (red dashed box in Fig. 1) including the AC/DC converter. The PV array (in Fig. 2) is implemented as a five-parameter model (in terms of a dependent current source I_l, a diode D, a series resistance R_s, and a shunt resistance R_{sh}) to simulate the nonlinear irradiance- and temperature-dependent current-voltage (I-V) characteristics in the PV system. The AC/DC converter contains a bank of insulated-gate bipolar transistors (IGBTs) in an *H-bridge* topology which uses PWM signals received from the controller. As shown in Fig. 2, the considered loads include "Load 1" and "Load 2" which are 50 kW and 100 kW, respectively.

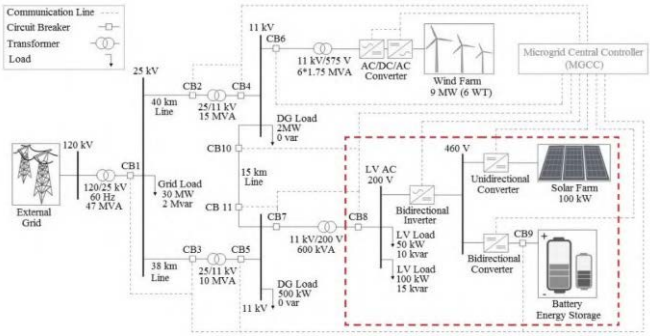

Fig. 1. Diagram of the microgrid under consideration.

3. PHOTOVOLTAIC SYSTEM POWER-LOSS SCENARIO

Microgrid is obviously a highly nonlinear complex system with various distributed components which needs to operate in a safe and reliable way. However, faults may happen at various locations of this system in any forms of sensor, actuator or component faults. As a general solution in the event of faults inside a microgrid, the protective devices need to disconnect the smallest possible section of the microgrid in order to clear the fault and prevent its effects from propagating within the whole system. As a fault happens outside the microgrid (in the external grid), the microgrid can be disconnected/isolated from the external grid, and the system transforms into the islanded operation mode. However, thanks to the strong coupling between the operations of different units inside a microgrid, the presence of a hierarchical control scheme together with the possibility of coordination between local controllers, some types of faults can be effectively tolerated and accommodated using FTC methods at the control system level without any unnecessary disconnections.

In a PV array, faults can specifically occur in cell, module and bypass diodes due to overheating, damaged panels, or open/short circuits. In addition, debris accumulation on the panel surface is considered as another source of fault in PV systems. These failure modes result in an abnormal reduction in the PV output power. Accordingly, a sudden imbalance between loads' demanded power and the PV generated power happens which comes with unwanted variations in the voltage and current waveforms together with frequency deviations for the AC part of hybrid AC/DC microgrid.

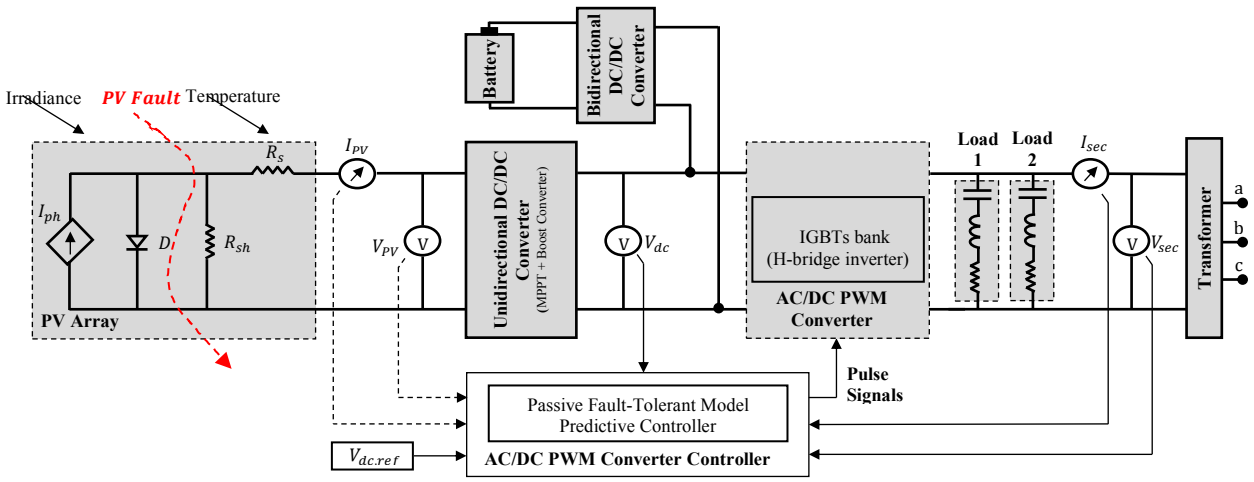

Fig. 2. Schematic of the implemented DC part of the microgrid.

Indeed, any sudden reduction in the PV output power causes adverse impacts on the quality of current, voltage, as well as the stability of frequency and voltage all-over the microgrid.

In the considered benchmark, a bidirectional AC/DC converter is responsible for connecting the DC part to the AC part in the microgrid. This converter is equipped with a bank of IGBTs which exploits PWM signals to convert and regulate the power flow, and maintain the DC bus voltage at 460 volts (V). A severe power-loss fault in the PV array will adversely affect the output signals of the PV system, the stability of the DC bus voltage, the active and reactive power flows through CB8 (in Fig. 1), and the microgrid's frequency in its AC part. However, as shown in Sections 4 and 5, a well-designed FTC system for the AC/DC converter can effectively maintain the reliable operation of microgrid under such power-loss faults with an acceptable performance.

4. PASSIVE FAULT-TOLERANT MODEL PREDICTIVE CONTROL DESIGN

Power electronic converters are required to integrate the PV array into the hybrid AC/DC microgrid. As already mentioned, an AC/DC PWM converter and a unidirectional DC/DC converter (MPPT controller and a boost converter) is used here to regulate the power flow and stabilize the system as loads change. Figure 3 shows the control loop of the AC/DC converter which uses the secondary voltage and current of the transformer and high DC voltage as feedback signals to maintain the DC bus voltage within a safe range. By default, the converter uses a PWM signal generator, and two PI controllers in a feedforward path. According to Ziegler-Nichols tuning technique, the control gains are $\{K_{p,1} = 300, K_{I,1} = 3{,}500\}$ and $\{K_{p,2} = 0.1, K_{I,2} = 25\}$ for the first and second PI controllers, respectively. This paper aims at designing a PFTC scheme based on MPC algorithm for the first controller to substitute the baseline PI controller and enable the accommodation of the PV power-loss fault effects in the microgrid. As can be seen, the default AC/DC PWM converter controller uses measured voltages and current signals (V_{dc}, V_{sec}, I_{sec}) as feedback to generate pulse signals for the IGBTs, while the designed PFTCs need two extra feedback signals from the PV outputs V_{PV} and I_{PV} (dashed arrows in Fig. 3). These inputs allow for better understanding of the system dynamics, and provide some level of predictability of system behavior to facilitate PFTC design.

In MPC method, an optimal control problem will be solved over a limited horizon at each time step using the current state. For the next sampling time, the computation should be done again starting from the new state over a shifted horizon. The solution depends on a linear model, considered constraints, and optimization of a quadratic cost function. Therefore, the designed MPC provides near-optimal performance if the model is accurate enough and the quadratic cost function and specified constrains can express the true performance objectives. In addition to the model, performance index and constraints, the MPC method uses a state estimator to obtain the true states of the model. The following sections provide more details about the proposed MPC scheme.

4.1 Prediction Model

The model used in the MPC for prediction and state estimation is illustrated in Fig. 4. This linear time invariant (LTI) system includes the model of the plant under control whose inputs are the manipulated variable (MV), the root mean square (RMS) value of the secondary voltage and current, and the output voltage and current of the PV array.

All calculations related to the MPC are performed using a discrete-time state-space system. The plant model is an LTI discrete-time system described by Bemporad et al. (2004)

$$\begin{cases} x_p(k+1) = A_p x_p(k) + B_{p,mv} u(k) + B_{p,v} u_v(k) \\ y_p(k) = C_p x_p(k) + D_{p,mv} u(k) + D_{p,v} u_v(k) \end{cases} \quad (1)$$

where $A_p(k)$, $B_{p,mv}(k)$, $B_{p,v}(k)$, $C_p(k)$, $D_{p,mv}(k)$, and $D_{p,v}(k)$ are constant state-space matrices. Also, $x_p(k)$, $u(k)$, $u_v(k)$ and $y_p(k)$ are the state vector, manipulated variables, measured inputs and the output vector of the plant model, respectively. In the designed controller, the plant model is linearized as a third order system in which the inputs are $u(k)$ and $u_v(k) = [I_{s,RMS}, V_{s,RMS}, I_{PV}, V_{PV}]^T$; and the output is the high DC voltage $y(k) = V_{dc}(k)$. This model for MPC is accurate enough to capture the most significant dynamics of the microgrid during fault-free and faulty operation.

The output disturbance model is used for optimisation and its output $y_{od}(k)$ is added to the plant output. To reject constant disturbances, due to single-phase load changes in the microgrid, the output disturbance model is a collection of integrators driven by white noise as the following form

$$\begin{cases} x_{od}(k+1) = A_{od} x_{od}(k) + B_{od} u_{od}(k) \\ y_{od}(k) = C_{od} x_{od}(k) + D_{od} u_{od}(k) \end{cases} \quad (2)$$

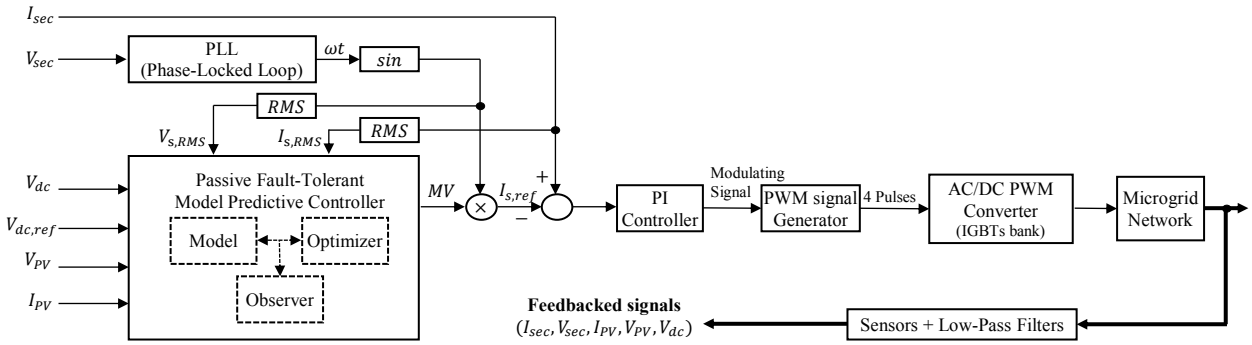

Fig. 3. Block diagram of the AC/DC PWM converter control loop with model predictive controller.

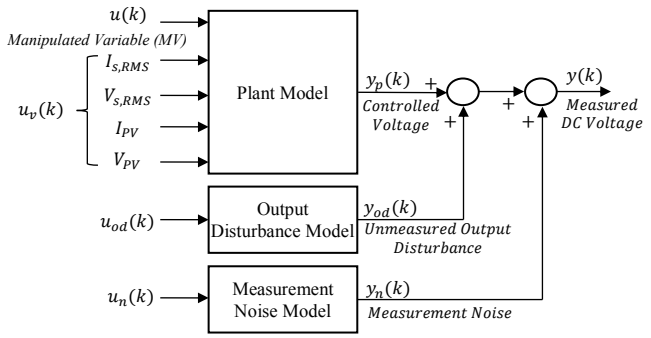

Fig. 4. Model structure used in MPC controller for prediction and state estimation.

where $A_{od}(k)$, $B_{od}(k)$, $C_{od}(k)$, and $D_{od}(k)$ are constant state-space matrices, and $x_{od}(k)$, $u_{od}(k)$ and $y_{od}(k)$ are the disturbance model state vector, white noise inputs (with unit variance) and the output disturbances, respectively.

In order to distinguish disturbances from measurement noise, a model for measurement noise is also described as a discrete-time LTI model by

$$\begin{cases} x_n(k+1) = A_n x_n(k) + B_n u_n(k) \\ y_n(k) = C_n x_n(k) + D_n u_n(k) \end{cases} \tag{3}$$

where $A_n(k)$, $B_n(k)$, $C_n(k)$, and $D_n(k)$ are constant state-space matrices, and $x_n(k)$, $u_n(k)$ and $y_n(k)$ are the state vector, white noise inputs and noise model output signals to be added to the plant outputs, respectively.

4.2 Optimization Problem

In MPC, an optimization problem (a quadratic programing (QP)) is solved at each control interval. The manipulated variables (MVs) that will apply to the plant until the next control interval are determined. Normally, the cost function is the sum of four terms to focus on particular aspects of the controller design: output tracking, manipulated variable tracking, small MV moves, and constraint. MPC method employs a nonnegative slack variable ε_k which quantifies the worst-case constraint violation. Overall, each term uses appropriate weights to balance designed objectives. The smaller weight corresponds to the less important term of the overall cost function.

In general, the controller states are unmeasured and must be estimated. A *steady-state Kalman filter* that derives from the state observer is used by MPC controller. The following optimization problem is used to obtain the control action at time k (note that the states of the model at time k are available from the Kalman filter):

$$\begin{aligned} J(Z_k) = \sum_{i=0}^{p-1} \Bigg(& \sum_{j=1}^{n_y} \Big(w_{i+1,j}^{y} \big[y_j(k+i+1|k) \\ & - r_j(k+i+1|k) \big] \Big)^2 \\ & + \sum_{j=1}^{n_u} \Big(w_{i,j}^{u} \big[u_j(k+i|k) \\ & - u_{j,target}(k+i|k) \big] \Big)^2 \\ & + \sum_{j=1}^{n_u} \Big(w_{i,j}^{\Delta u} \big[u_j(k+i|k) \\ & - u_j(k+i-1|k) \big] \Big)^2 \Bigg) + \rho_\varepsilon \varepsilon_k^2 \end{aligned} \tag{4}$$

where '$(.)_j$' represents the jth component of a vector, '$(k+i|k)$' means the value predicted at time-step $k+i$ based on the information available at k. Moreover, $y_j(k+i+1|k)$ is the predicted value of jth output at $(i+1)$th prediction step, $r_j(k+i+1|k)$ is the reference value for the mentioned output at $(i+1)$th step, $u_{j,target}(k+i|k)$ is the target value for jth MV, $w_{i+1,j}^{y}$ is the weight for jth output at $(i+1)$th step, $w_{i,j}^{u}$ is the weight for jth MV at ith step, and $w_{i,j}^{\Delta u}$ is the weight for jth MV movement at ith step. Z_k is the QP decision as

$$Z_k^T = [\Delta u(k|k)^T \quad \Delta u(k+1|k)^T \quad \dots \quad \Delta u(k+m-1|k)^T \quad \varepsilon_k]$$

with k current control interval, p prediction horizon, m control horizon, n_y number of plant output variables, and n_u number of manipulated variables.

It should be noted that $u_{j,target}(k+i|k)$ values are available for the entire horizon. Also, the plant outputs $y_j(k+i+1|k)$ are predicted by the state observer. At time-step k, the estimation of the controller state and measured inputs are available. Accordingly, J is only a function of Z_k. MPC constraints are defined as follows:

$$\begin{aligned} y_{j,min}(i) - \varepsilon_k V_{j,min}^{y}(i) \le y_j(k+i+1|k) \\ \le y_{j,max}(i) - \varepsilon_k V_{j,max}^{y}(i), \\ j = 1, \dots, n_y \end{aligned} \tag{5}$$

$$\begin{aligned} u_{j,min}(i) - \varepsilon_k V_{j,min}^{u}(i) \le u_j(k+i|k) \\ \le u_{j,max}(i) - \varepsilon_k V_{j,max}^{u}(i), \\ j = 1, \dots, n_u \end{aligned} \tag{6}$$

$$\begin{aligned} \Delta u_{j,min}(i) - \varepsilon_k V_{j,min}^{\Delta u}(i) \le \Delta u_j(k+i|k) \\ \le \Delta u_{j,max}(i) - \varepsilon_k V_{j,max}^{\Delta u}(i), \\ j = 1, \dots, n_u \end{aligned} \tag{7}$$

$$\Delta u(k+h|k) = 0 \tag{8}$$

$$\varepsilon_k \ge 0 \tag{9}$$

for all $i = 0, \dots, p-1$, $h = m, \dots, p$ and with respect to the input increments $\{\Delta u(k|k), \dots, \Delta u(k-1+m|k)\}$ and the slack variable ε_k. The controller uses $u(k) = u(k-1) + \Delta u^*(k|k)$ in which $\Delta u^*(k|k)$ is the first term of the optimal sequence. In the above equations, $y_{j,min}(i)$ and $y_{j,max}(i)$ are the lower and upper bounds for jth output at ith step, $u_{j,min}(i)$ and $u_{j,max}(i)$ are the lower and upper bounds for jth MV at ith step, and $\Delta u_{j,min}(i)$ and $\Delta u_{j,max}(i)$ are the lower and upper bounds for jth MV increment at ith step. Also, V parameters are controller constants that are used for constraint softening. By default, all the input constraints are chosen to be hard and all the output constraints are soft. As already mentioned, only $\Delta u(k|k)$ is used to compute manipulated variable. The remaining samples $\Delta u(k+i|k)$ are discarded and a new optimization problem is solved at the next time-step.

5. SIMULATION RESULTS

In this section, the simulation results are presented to demonstrate the effectiveness of the proposed PFTC scheme. The benchmark model presented in Section 2 is used, and the simulations are conducted over 4 seconds (sec) in MATLAB/Simulink environment. The reference value for the high DC voltage is set to be constant at 460 V during the microgrid operation in its grid-connected mode. The considered dynamic loads include "Load 1" that is active over time periods of [0.5,1.5] sec and [2.5,3.5] sec, and "Load 2" that is active during [1.0,1.5] sec and [3.0,3.5] sec. It is assumed that the loads are supplied using the PV system if possible, or by receiving an extra power from the AC part of the microgrid if more power is needed. Also, the BESS only connects when CB8 trips open (see Fig. 1).

A power-loss fault in the PV system is simulated to begin from $t = 1$ sec and continue to the end of simulation $t = 4$ sec. During this time-period, the output power of the PV system is significantly decreased to about 35 percent of its nominal power. The PV output power in *fault-free operation* and *faulty operation* with the baseline PI controller are shown in Fig. 5. As can be seen, the output power of the PV array is suddenly reduced when the fault occurs at $t = 1$ sec.

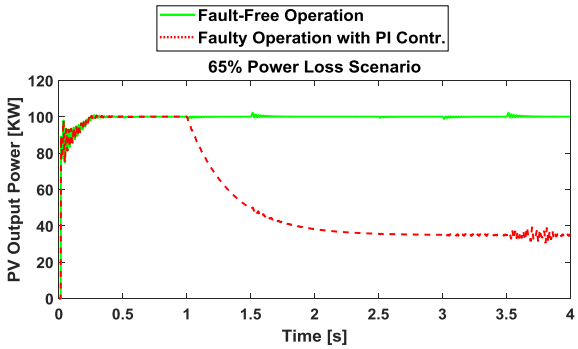

Fig. 5. PV output power during fault-free and faulty operation.

It is worth mentioning that any abrupt changes in microgrid operation, especially the connection and disconnection of dynamic loads during the fault events may destabilize the entire microgrid. Therefore, it is essential to carefully evaluate the effects of load variations on microgrid stability. Figure 5 clearly shows the effects of dynamic loads during faulty operation. One can observe that when Load 2 is disconnected (at 3.5 sec), the PI controller cannot handle this disturbance under fault conditions and the output power starts to fluctuate.

Figure 6 shows the obtained high DC voltage signal around the reference value of $V_{dc,ref} = 460$ V. Maintaining this high DC bus voltage within a safe range constitutes the major control objective during the microgrid operation. As shown in Fig. 6, using the baseline PI controller, this voltage adversely deviates from its reference value, while the PFTC scheme can effectively maintain the voltage throughout the simulation under both fault conditions and severe load disturbances. The inferior performance of PI controller in Fig. 6 is especially obvious from $t = 2.5$ sec when the fault is fully developed and Load 1 is connected to the microgrid.

Figure 7 shows power consumptions by Load 1 and Load 2 around $t = 3$ sec. As observed, the proposed PFTC scheme scores a better performance compared with that of the baseline PI controller.

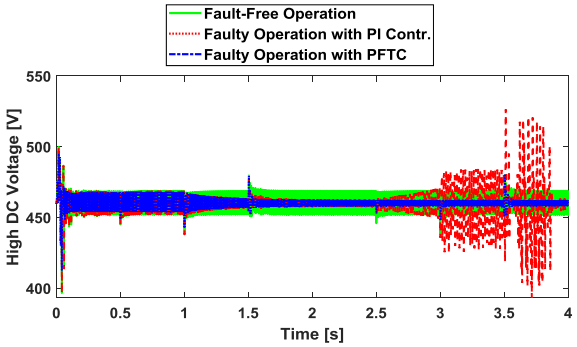

Fig. 6. High DC voltage.

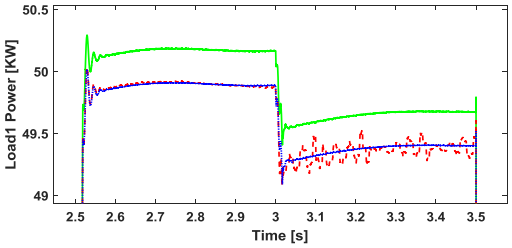

(a)

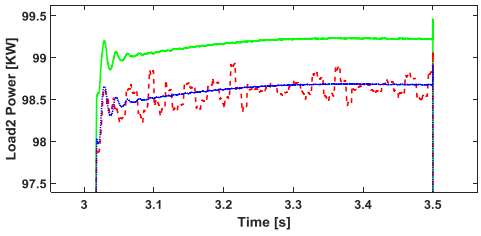

(b)

Fig. 7. Load powers: (a) Load1 from 2.5 to 3.5 sec., (b) Load 2 from 3 sec to 3.5 sec.

As already mentioned, the AC/DC PWM converter is responsible for regulating the power flow between the microgrid's DC and AC parts. Figure 8 shows the transmitted active and reactive powers through CB8. The negative amounts of active power represent the power received from the grid. As shown in the figure, when the PV power-loss fault increases in magnitude, more active power is received from the grid. One can see that the baseline PI controller only handles small (mild) amounts of power-loss fault, while the proposed PFTC scheme exhibits a robust performance all the time.

Although the considered fault occurs inside the DC part of microgrid, the AC part is also affected. Figure 9 shows the

microgrid frequency measured by a phasor measurement unit (PMU) at "11 kV bus" (see Fig. 1). All simulation results show the effectiveness of the proposed PFTC scheme in both fault-free and faulty conditions for the microgrid under the considered dynamic loads.

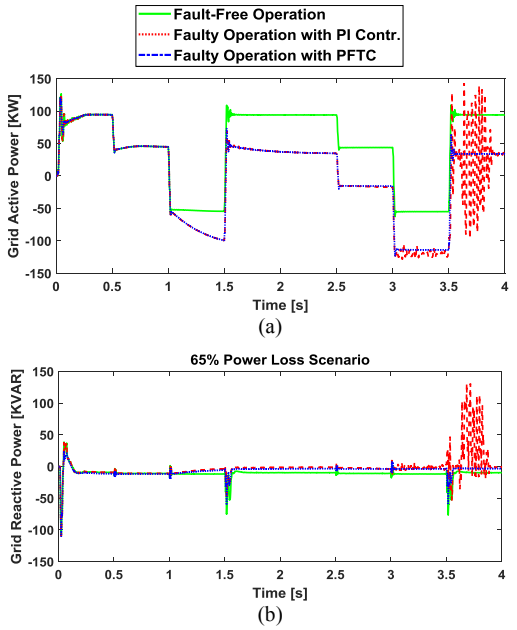

Fig. 8. CB8 power flow: (a) active power, (b) reactive power.

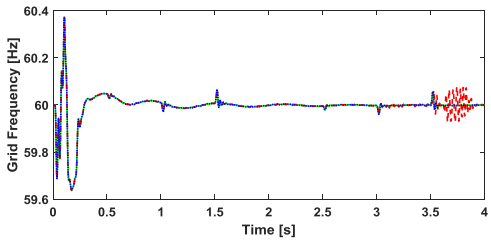

Fig. 9. Measured frequency at 11 kV bus.

6. CONCLUSIONS

In this paper, a cluster of distributed renewable energy resources, battery energy storage, and dynamic loads are considered to form a hybrid AC/DC microgrid. A passive fault-tolerant control scheme based on model predictive control is designed at the power electronic level to accommodate possible power-loss faults in the PV system. This is done without requiring any explicit information of faults (i.e., no need for fault detection and diagnosis).

An advanced microgrid benchmark with dynamic loads and a wide range of operating conditions is modeled in MATLAB/Simulink environment. According to the simulation results, the proposed control scheme scores a robust performance in the presence of both severe power-loss faults and abrupt variations in dynamic loads.

Extending the proposed approach to the accommodation of other types of faults (such as converter faults or sensor faults in the presented hybrid microgrid) remains one of the future works. Also, to obtain better results, other advanced control techniques such as adaptive controllers or multiple MPC controllers for multiple operating points can be explored in the future.

REFERENCES

Badihi, H., Jadidi, S., Zhang, Y.M., Su, C.Y., and Xie, W.F., (2019). AI-Driven Intelligent Fault Detection and Diagnosis in a Hybrid AC/DC Microgrid. *IEEE 1st International Conference on Industrial Artificial Intelligence (IAI)*, pp. 1-6.

Bemporad, A., Ricker, N., Owen, J.G. (2004). Model Predictive Control-New tools for design and evaluation. *American Control Conference IEEE*, 6, pp. 5622-5627.

Gholami, S., Saha, S., Aldeen, M. (2018). Fault tolerant control of electronically coupled distributed energy resources in microgrid systems. *International Journal of Electrical Power & Energy Systems,* 95, pp. 327-340.

Jadidi, S., Badihi, H., Zhang, Y.M. (2019a). A review on operation, control and protection of smart microgrids. *IEEE 2nd International Conference on Renewable Energy and Power Engineering (REPE)*, pp. 100-104.

Jadidi, S., Badihi, H., Zhang, Y.M. (2019b). Passive fault tolerant control of PWM converter in a hybrid AC/DC microgrid. *IEEE 2nd International Conference on Renewable Energy and Power Engineering (REPE)*, pp. 90-94.

Khosravani, S., Moghaddam, I.N., Afshar, A. and Karrari, M. (2016). Wide-area measurement-based fault tolerant control of power system during sensor failure. *Electric Power Systems Research*, 137, pp. 66-75.

Lasseter, B. (2001). Microgrids [distributed power generation]. *Power Engineering Society, IEEE,* 1, pp. 146-149.

Minchala-Avila, L.I., Vargas-Martinez, A., Garza-Castanon, L.E., Morales-Menendez, R., Zhang, Y.M., and Calle Ortiz, E.R. (2014). Fault-tolerant control of a master generation unit in an islanded microgrid. *IFAC Proceedings,* 47(3), pp. 5327-5332.

Prodan, I., Zio, E. and Stoican, F. (2015). Fault tolerant predictive control design for reliable microgrid energy management under uncertainties. *Energy,* 91, pp. 20-34.

Tremblay, O. and Dessaint, L.A. (2009). Experimental validation of a battery dynamic model for EV applications. *World Electric Vehicle Journal,* 3, pp. 289-298.

Youssef, F.B. and Sbita, L. (2017). Sensors fault diagnosis and fault tolerant control for grid connected PV system. *International Journal of Hydrogen Energy*, 42(13), pp. 8962-8971.